Preparation of Polycrystalline TiO_2 Photocatalysts Impregnated with Various Transition Metal Ions: Characterization and Photocatalytic Activity for the Degradation of 4-Nitrophenol

A. Di Paola,[†] G. Marcì,[†] L. Palmisano,*[,†] M. Schiavello,[†] K. Uosaki,[‡] S. Ikeda,[§] and B. Ohtani[§]

Dipartimento di Ingegneria Chimica dei Processi e dei Materiali, Università di Palermo, Viale delle Scienze, 90128 Palermo, Italy, Physical Chemistry Laboratory, Division of Chemistry, Graduate School of Science, Hokkaido University, Sapporo 060-0810, Japan, and Catalysis Research Center, Hokkaido University, Sapporo 060-0811, Japan

Received: August 9, 2001

A set of polycrystalline TiO_2 photocatalysts loaded with various ions of transition metals (Co, Cr, Cu, Fe, Mo, V, and W) were prepared by using the wet impregnation method. The samples were characterized by using some bulk and surface techniques, namely X-ray diffraction, BET specific surface area determination, scanning electron microscopy, point of zero charge determination, and femtosecond pump−probe diffuse reflectance spectroscopy (PP-DRS). The samples were employed as catalysts for 4-nitrophenol photodegradation in aqueous suspension, used as a probe reaction. The characterization results have confirmed the difficulty to find a straightforward correlation between photoactivity and single specific properties of the powders. Diffuse reflectance measurements showed a slight shift in the band gap transition to longer wavelengths and an extension of the absorption in the visible region for almost all the doped samples. SEM observation and EDX measurements indicated a similar morphology for all the particles, and a not homogeneous distribution of the metal species onto the surface of catalyst particles. The impregnated samples revealed recombination rates always higher than that of bare TiO_2. The photoactivity of TiO_2 was reduced by the presence of transition metal ions with the exception of W, which instead played a beneficial role. The results of femtosecond pump−probe diffuse reflectance spectroscopy appear quite in accord with the observed photocatalytic activity only for the lowest values of electron−hole recombination rate of the samples.

Introduction

Doping with suitable transition metal ions allows extending the light absorption of large band gap semiconductors to the visible region.[1−8] Also, metals belonging to group VIII, as for instance Pd and Pt, have been deposited onto the surface of semiconductors to improve the separation of photogenerated electron−hole pairs.[9−14] These methods have been used with the aim to enhance the photocatalytic activity both in gas−solid and in liquid−solid systems.

TiO_2 is the most used and popular photocatalyst for various reasons, but unfortunately, although a large shift of light absorption in the visible region has been observed in almost all cases, the presence of dopant metal species has not been reported beneficial when photooxidation reactions of organic substrates in aqueous systems were carried out,[15−18] with the exception of tungsten ions in particular amounts.[5,6] Some authors have reported[19] that the recombination rate of the electron−hole pairs increases for chromium-doped TiO_2 with respect to undoped TiO_2, and others suggest a correlation between the lifetime of the charge carriers and the photocatalytic activity for samples doped with Cr^{3+} and Mo^{5+} ions.[20] A higher diffusion length of the minority carriers for iron ion doped TiO_2 with respect to undoped TiO_2 has been also determined.[21]

The dopants are usually confined as very dispersed species to the surface and/or to a few top layers of TiO_2 particles, due to the moderate calcination temperatures used in the conventional preparations. Very recently[22,23] the expensive ion implantation method has been used to obtain photocatalysts more active than the corresponding bare TiO_2. In this case ions are believed to be present in substitutional positions in the lattice of TiO_2, and a change of the band-gap energy may occur in addition to an extension of light absorption in the visible region.

A comparison among the results reported in the literature for doped samples obtained from various preparations is not easy because the experimental conditions under which the runs are carried out and the preparation methods of the samples are usually different.[9] Moreover, it is well known that bare polycrystalline anatase and rutile TiO_2 samples also show very different photoactivities, depending on their electronic and surface physicochemical properties.[9,24−27] Nevertheless, it is worth pointing out that the photoactivity cannot be straightforwardly related to only few properties because it depends on all of them. Therefore, to compare the photoactivity of variously doped TiO_2 samples, it would be necessary to use the same bare TiO_2 as the starting material by scrutinizing carefully the various insights deriving from the characterization results and to evaluate their relative importance.

In this paper it is reported the preparation of TiO_2 polycrystalline powders loaded with some transition metal ions (chromium, cobalt, copper, iron, molybdenum, tungsten, and vanadium) by using the incipient wet impregnation method. The samples have been characterized by X-ray diffractometry

* Corresponding author.
[†] Università di Palermo.
[‡] Graduate School of Science, Hokkaido University.
[§] Catalysis Research Center, Hokkaido University.

10.1021/jp013074l CCC: $22.00
Published on Web 12/28/2001

(XRD), specific surface area determinations, measurements of the point of zero charge (pzc), scanning electron microscopy (SEM) coupled with electron microprobe used in an energy-dispersive mode (EDX), and femtosecond pump−probe diffuse reflectance spectroscopy (PP-DRS). The photoactivity of the samples was tested for 4-nitrophenol photodegradation in aqueous medium,[28,14] chosen as a probe reaction.

Experimental Section

Catalysts Preparation. Bare TiO_2 was prepared in an open reactor by reacting 1 L of titanium trichloride (Carlo Erba RPE, gravimetric title 15%) with 0.8 L of ammonia (Carlo Erba RPE, gravimetric title 25%) diluted in 0.5 L of bidistilled water. The powdered titanium hydroxide obtained was washed several times in order to eliminate the chloride ions, dried 24 h at 373 K, and heated in air for 24 h at 773 K. This sample was denoted as TiO_2 HP.

Samples containing 0.3, 1.0, 2.0, and 5.0 moles of metal ions over 100 moles of metal and titanium ions were prepared by the wet impregnation method. TiO_2 HP was impregnated with aqueous solutions containing the required amounts of the transition metal ions, i.e., $Co(NO_3)_2 \cdot 6H_2O$, $Cr(NO_3)_3 \cdot 9H_2O$, $Cu(NO_3)_2 \cdot 3H_2O$, $Fe(NO_3)_3 \cdot 9H_2O$, $(NH_4)_6Mo_7O_{24} \cdot 4H_2O$, NH_4VO_3, and $(NH_4)_6W_{12}O_{39}.xH_2O$ (85 wt % WO_3).

After standing at room temperature for 24 h, water was evaporated by heating the samples at 373 K for 24 h. Subsequently, the dried solids were fired in air at 773 K for 24 h. The final powders were denoted by using the following code: TiO_2/Me/X, where Me indicates the kind of metal ion and X its molar percentage.

X-ray Diffraction. The XRD patterns of the powders were collected at room temperature by a Philips powder diffractometer using Cu Kα radiation and a 2θ scan rate of 2°/min.

Diffuse Reflectance Spectroscopy. Diffuse reflectance spectra were recorded by means of a Shimadzu UV-2401 PC instrument, using $BaSO_4$ as reference sample. The spectra were recorded at room temperature in air, in the range 200−800 nm.

Specific Surface Area Measurements. The specific surface areas were determined by the single-point BET method[29] using a Flow Sorb 2300 apparatus (Micromeritics).

Scanning Electron Microscopy Observation and Energy Dispersive X-ray Analysis. SEM was performed using a model 505 Philips microscope, operating at 25 kV on specimens upon which a thin layer of gold or carbon had been evaporated. An electron microprobe used in an EDX mode was employed to obtain quantitative information on the amount and distribution of the metal species in the samples.

Point of Zero Charge Determination. The point of zero charge (pzc) of the samples was determined by the method of mass titration. This procedure has been described by Noh and Schwarz[30,31] and involves finding the asymptotic value of the pH of an oxide/water slurry as the oxide mass content is increased. Varying amounts of powders were added to water, and the resulting pH values were measured after 24 h of equilibration. Typical values of oxide/water by weight were 0.1, 1, 5, 10, 20, and 40%.

Femtosecond Pump−Probe Diffuse Reflectance Spectroscopy. Details of the time-resolved spectroscopy have been reported.[14] A brief summary of the procedures is as follows. A light pulse source consists of a mode-locked Ti:sapphire laser (Spectra-Physics, Tsunami: 3960-L2S) pumped by an argon ion laser (Spectra-Physics, BeamLok: 2580C) with a regenerative amplifier system (Quantronix, 4812RGA/4823S/C), which was synchronously pumped by a mode-locked YLF laser (Quantronix, 527DP−H). The final output consisting of ca. 100 fs pulses (1 kHz) was split into two beams with almost same the intensities in order to pump two identical optical parametric generation (OPG)/optical parametric amplification (OPA) systems (Light Conversion, TOPAS). One 620-nm output beam was used as a probe beam (1.5 mJ/pulse), and another was frequency-doubled in a BBO crystal to use as a pump beam (0.1−0.03 mJ/pulse). The pump and probe beams were collinearly focused and overlapped at the sample, and the diffusely reflected probe beam was measured in air at ambient temperature. Reflectance data were accumulated and recorded as absorption, $(R_0 - R)/R_0$, where R_0 and R are reflection intensity before and after the pump pulse, respectively.

Apparatuses and Procedures for the Photoreactivity Tests. A Pyrex batch photoreactor of cylindrical shape containing 0.5 liters of aqueous suspension was used. The photoreactor was provided with ports in its upper section for the inlet and outlet of gases, for sampling, and for pH and temperature measurements. A 125 W medium-pressure Hg lamp (Helios Italquartz, Italy) was immersed within the photoreactor. The photon flux emitted by the lamp, $\Phi_i = 13.5$ mW cm^{-2}, was measured using a radiometer (UVX Digital) leaned against the external wall of the photoreactor containing only pure water. Oxygen was continuously bubbled into the suspensions for ca. 0.5 h before switching on the lamp and throughout the occurrence of the photoreactivity experiments. The amount of catalyst used for all the experiments was 1.4 g L^{-1}, and the initial 4-nitrophenol (BDH) concentration was 20 mg L^{-1}. The initial pH of the suspension was adjusted to 4.5 by addition of H_2SO_4 (Carlo Erba RPE), and the temperature inside the reactor was ca. 300 K. The photoreactivity runs lasted 6.0 h, including the first half hour during which the lamp was switched off. Samples of 5 mL volume were withdrawn from the suspensions every 30 or 60 min, and the catalysts were separated from the solution by filtration through 0.45 mm cellulose acetate membranes (HA, Millipore). The quantitative determination of 4-nitrophenol was performed by measuring its absorption at 315 nm with a spectrophotometer Beckman DU 640. Total organic carbon (TOC) determinations were carried out by using a TOC 5000 A Shimadzu analyzer.

Results

X-ray Diffraction Analysis. The XRD patterns of TiO_2 HP showed a mixture of anatase and rutile[33] in the ratio of ca. 4:1, determined by the intensities obtained from the areas of the most intense diffraction peaks due to these two modifications of titania.[34] This composition remained constant after a further thermal treatment for 24 h at 773 K.

The diffraction patterns of the doped powders were almost coincident with those of TiO_2 HP. As shown in Figures 1 and 2, only the diagrams of a few samples with the highest metal content (TiO_2/Co/5, TiO_2/Cu/5, and TiO_2/W/5) showed very small peaks attributable to separate oxide phases, in addition to the lines of TiO_2. In particular, the diffractogram of TiO_2/W/5 revealed clearly weak peaks corresponding to the monoclinic WO_3 phase.[35]

The intensity of the peaks of rutile decreased in the presence of Cr (diffractogram not shown for the sake of brevity) and increased if the samples contained Co or Cu. As revealed by Figure 2, the Fe-doped specimen presented less anatase than the bare TiO_2, while the peaks of TiO_2/V/5 were narrower than those of the TiO_2 precursor.

Diffuse Reflectance Measurements. Visible-ultraviolet spectra of loaded and bare TiO_2 were obtained by diffuse reflectance

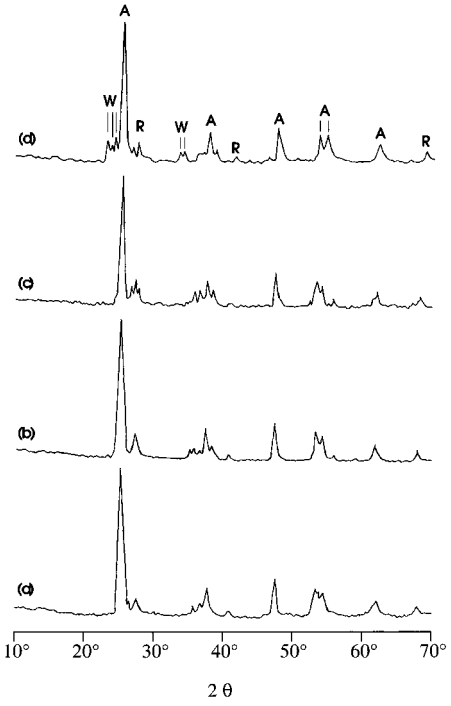

Figure 1. X-ray diffraction patterns of TiO_2 and various samples containing 5% of transition metal: (a) TiO_2 HP, (b) TiO_2/Co, (c) TiO_2/Cu, (d) TiO_2/W. A: anatase, R: rutile, W: WO_3.

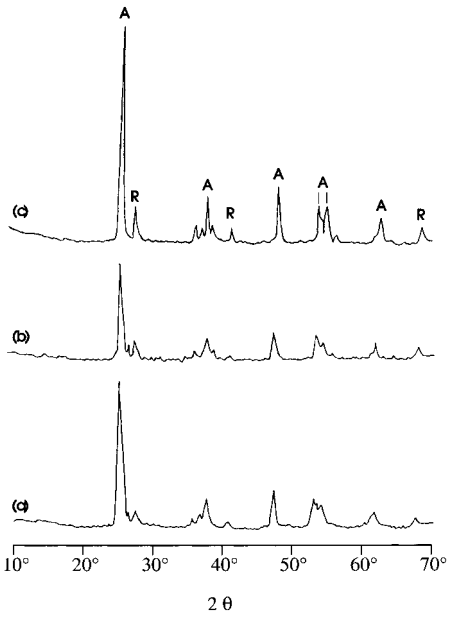

Figure 2. X-ray diffraction patterns of TiO_2 and various samples containing 5% of transition metal: (a) TiO_2 HP, (b) TiO_2/Fe, (c) TiO_2/V. A: anatase, R: rutile.

spectroscopy. Representative examples are given in Figure 3. The spectra of the loaded samples showed a slight shift in the band gap transition to longer wavelengths, the extent depending on the amount of metal loading. The absorbance in the visible region was always higher than that of TiO_2 and, in particular, the most pronounced effect occurred in the case of the co-loaded powders. The spectra of the samples containing tungsten were little affected by the presence of the loading metal.

Specific Surface Area Measurements and Scanning Electron Microscopy Observations. The specific surface areas of the various samples are reported in Table 1. The areas of the powders loaded with Co, Cr, Fe, Mo, and W ions were very similar to that of TiO_2, especially for low contents of metal. As the amount of metal increased, the specific surface areas decreased. This effect was significantly evident for the TiO_2/Cu and TiO_2/V samples, and in particular the surface areas of TiO_2/Cu/5 and TiO_2/V/5 were ca. 30% lower than that of TiO_2 HP. The areas of the various Mo−TiO_2 samples were practically identical to each other.

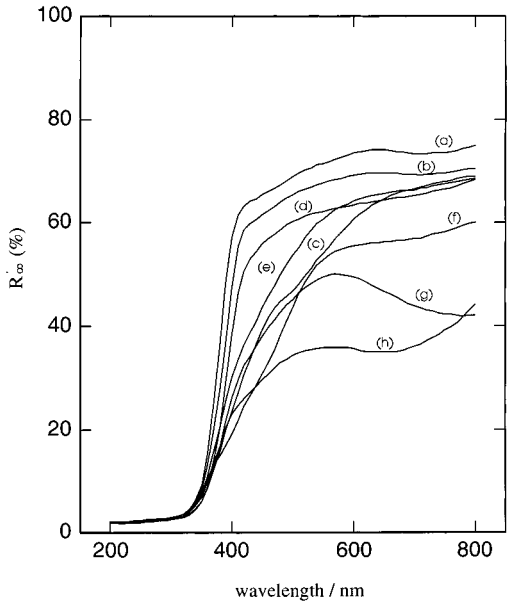

Figure 3. Visible-UV spectra (diffuse reflectance) of TiO_2 and doped samples containing 1% of transition metal: (a) TiO_2 HP, (b) TiO_2/W, (c) TiO_2/Fe, (d) TiO_2/Mo, (e) TiO_2/V, (f) TiO_2/Cr, (g) TiO_2/Cu, (h) TiO_2/Co.

TABLE 1: Specific Surface Areas (SSA), Points of Zero Charge (pzc), Observed Rate Constants of 4-nitrophenol Photodegradation (r_0 and r'_0) and Second-order Rate Constants of Electron−Hole Recombination, k_r

sample	SSA ($m^2\,g^{-1}$)	pzc (pH)	$r_0 \times 10^{10}$ (mol $L^{-1}\,s^{-1}$)	$r'_0 \times 10^{10}$ [a] (mol $L^{-1}\,s^{-1}\,m^{-2}$)	k_r ($cm^3\,ps^{-1}$)
TiO_2 HP	61	7.1	1.9	4.4	1.4
TiO_2/Co/0.3	61	7.5	1.0	2.4	2.3
TiO_2/Co/1.0	57	7.7	0.9	2.3	2.5
TiO_2/Co/2.0	53	7.9	0.3	0.8	3.0
TiO_2/Co/5.0	51	8.5	0.2	0.6	-
TiO_2/Cr/0.3	61	3.6	0.8	1.9	2.8
TiO_2/Cr/1.0	58	3.3	0.5	1.2	2.3
TiO_2/Cr/2.0	57	2.5	0.3	0.8	3.4
TiO_2/Cr/5.0	53	2.0	0.1	0.3	-
TiO_2/Cu/0.3	61	7.3	1.4	3.2	2.2
TiO_2/Cu/1.0	56	7.6	1.0	3.1	2.3
TiO_2/Cu/2.0	47	8.2	1.0	3.0	2.5
TiO_2/Cu/5.0	42	8.9	0.7	2.4	-
TiO_2/Fe/0.3	61	7.2	1.1	2.6	2.6
TiO_2/Fe/1.0	58	7.4	0.8	2.0	4.1
TiO_2/Fe/2.0	56	7.7	0.7	1.8	4.6
TiO_2/Fe/5.0	53	8.1	0.2	0.5	4.8
TiO_2/Mo/0.3	61	7.4	1.1	2.6	1.8
TiO_2/Mo/1.0	59	5.8	1.6	3.9	2.1
TiO_2/Mo/2.0	62	3.9	1.0	2.3	5.2
TiO_2/Mo/5.0	63	2.2	0.5	1.1	-
TiO_2/V/0.3	60	7.4	0.7	1.7	1.9
TiO_2/V/1.0	52	5.4	0.4	1.1	3.1
TiO_2/V/2.0	49	3.6	0.3	0.9	3.7
TiO_2/V/5.0	41	2.7	0.2	0.7	-
TiO_2/W/0.3	61	7.0	1.7	4.0	2.3
TiO_2/W/1.0	60	6.6	2.7	6.4	1.9
TiO_2/W/2.0	58	5.7	2.5	6.2	2.3
TiO_2/W/5.0	54	2.8	1.7	4.5	2.2

[a] Values calculated by dividing r_0 by the surface area (obtained by multiplying the SSA for the amount of catalyst employed).

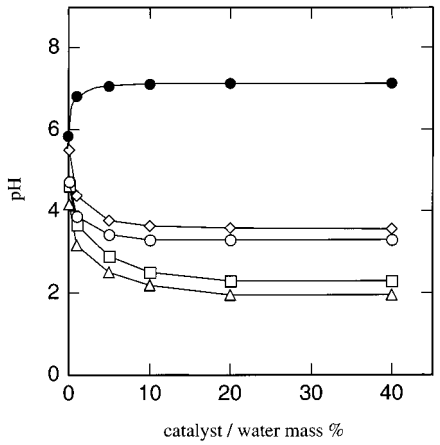

Figure 4. Plot of pH versus the catalyst/water mass percentage for TiO_2 and various TiO_2/Cr samples: (●) TiO_2 HP, (◇) TiO_2/Cr/0.3, (○) TiO_2/Cr/1.0, (□) TiO_2/Cr/2.0, (△) TiO_2/Cr /5.0.

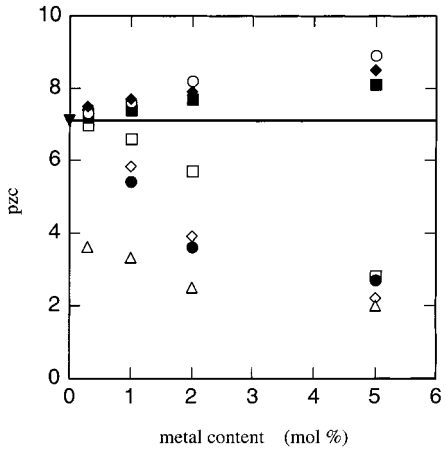

Figure 5. Points of zero charge of the various samples versus the amount of metal content. (▼) TiO_2 HP, (◆) TiO_2/Co, (△) TiO_2/Cr, (○) TiO_2/Cu, (■) TiO_2/Fe, (◇) TiO_2/Mo, (●) TiO_2/V, (□) TiO_2/W.

The SEM micrographs did not reveal significant morphological differences among TiO_2 HP and the loaded samples. The biggest particles appeared as aggregates with irregular shapes and sizes ranging between 20 and 100 μm. EDX analyses indicated that the mean atomic percentages of the various metals were quite similar to the nominal values with the exception of the V− and Mo−TiO_2 samples. In particular the percentages of vanadium were significantly lower than the nominal content, while those of Mo were always higher.

In all the samples, the distribution of loading metal on the single particles was not homogeneous and noticeable variations in the metal content were found in different particles or in different locations of the same particle.

Point of Zero Charge Measurements. The point of zero charge of the powders was estimated by using the method of mass titration,[30] which is an alternative to the widely used acid/base titration,[36,37] or to the pH drift technique.[37] The pH of the aqueous suspension of an oxide depends on the amount of oxide in a given volume of water, and the suspension pH often reaches a steady-state value after addition of excess solid: this limiting pH can be considered a reasonable estimate for the pzc of the oxide.[31] The procedure is to find the equilibrium pH where the addition of further amounts of oxide into the fresh solution does not affect the pH of the solution.

Figure 4 shows typical plots of pH versus mass percentage of oxide for TiO_2 HP and the powders loaded with Cr. The plateau in the mass titration curve is the pH corresponding to the pzc of the sample. Similar curves were obtained for all the samples.

The points of zero charge of the various powders are reported in Table 1. The value found for TiO_2 is in good agreement with those determined by other procedures.[31] However, it is worth noting that the differences found in the literature for similar samples can be due to specific adsorption of ions on the TiO_2 surface or to the presence of significant amounts of impurities in the oxide that contaminate the solid surface leading to a shift in the pH_{pzc}.[38]

The pzc values were plotted against the content of loading metal. As shown in Figure 5, the pzc of Cr, Mo, V, and W-loaded TiO_2 moves to a lower pH as the content of metal increases. In particular, for the Cr-loaded samples the equilibrium pH values are quite low, and an amount of ca. 0.3% of metal is enough to decrease the pzc of TiO_2 HP from 7.1 to 3.6. On the contrary, for Co, Cu, and Fe-doped TiO_2, the pzc moves to a value more basic than that of the support.

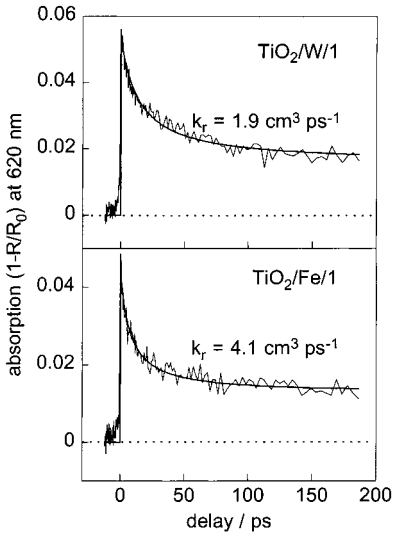

Figure 6. Representative decay profiles of transient absorption induced by ultrafast pump (ca. 100 fs). Results of TiO_2/W/1 and TiO_2/Fe/1 powders are shown.

Femtosecond Pump−Probe Diffuse Reflectance Spectroscopy. As already proven for TiO_2 powders and colloids,[39,40] the decay kinetics of photoexcited electrons trapped in surface sites reflects the recombination of electrons and positive holes. Femtosecond diffuse reflectance spectroscopy allows analyzing the charge recombination kinetics in the ultrafast time region.[40,41]

Figure 6 shows representative time profiles of various samples. The pump beam of wavelength at 310 nm induces a very rapid (< ca. 250 fs) rise of absorption at 620 nm, which is followed by a gradual decay. The latter decay part can be simulated on the assumption of a second-order kinetics of electron−hole recombination in the ps time scale.[42] The analysis of the decay curves allows estimating the rate constants of charge recombination, k_r (cm^3 ps^{-1}), which are summarized in Table 1.[14]

In Figure 7 the k_r values are plotted versus the content of loading metal. As reported previously,[14] the lowest values are exhibited by TiO_2 HP and by TiO_2/V/0.3, TiO_2/Mo/0.3, TiO_2/Mo/1, and TiO_2/W/1. All the other samples show recombination rates significantly higher than that of the support, and k_r generally increases with loading. It should be noted that the k_r values of the W-loaded samples are relatively low and are not much dependent on the content of metal. Moreover they are not much different from the k_r value of TiO_2 HP.

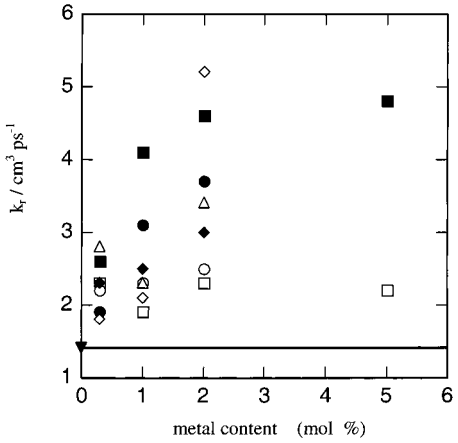

Figure 7. k_r values of TiO_2 and of the loaded samples versus the amount of metal content. Symbols are the same as in Figure 5.

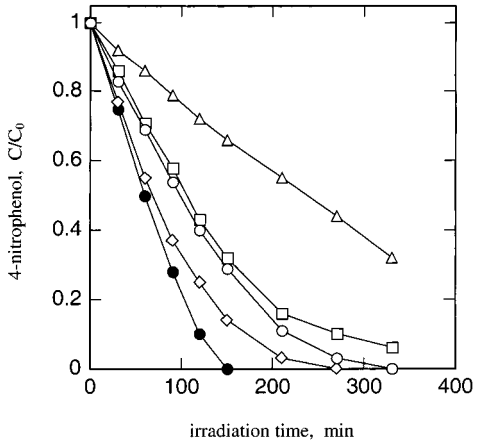

Figure 8. Photooxidation of 4-nitrophenol in the presence of TiO_2 and of Mo-loaded samples: (●) TiO_2 HP, (◇) TiO_2/Mo/0.3, (○) TiO_2/Mo/1.0, (□) TiO_2/Mo/2.0, (△) TiO_2/Mo/5.0.

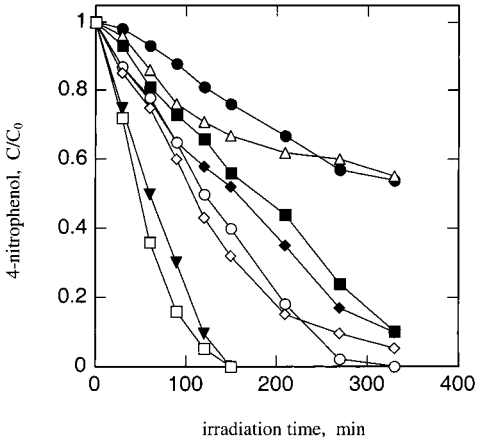

Figure 9. Photooxidation of 4-nitrophenol in the presence of TiO_2 and of various samples containing 1% of transition metal. Symbols are the same as in Figure 5.

Photoreactivity Results. The apparent kinetics of disappearance of 4-nitrophenol was followed by determining the concentration of the substrate at various time intervals. Figure 8 shows representative results for samples loaded with variable amounts of molybdenum.

Time required for the complete phototransformation of the substrate depended on the employed sample. Figure 9 summarizes the results of 4-nitrophenol oxidation in the presence of powders having the same percentage of different metals. The

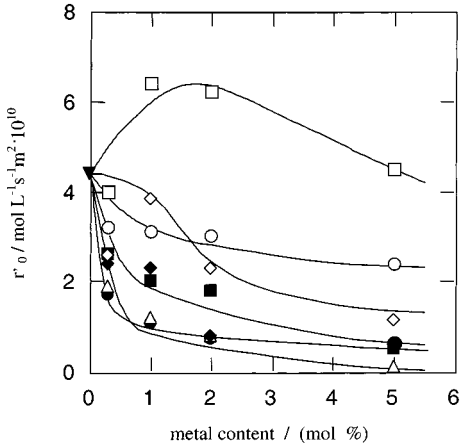

Figure 10. Plots of r'_0 versus the amount of metal content. Symbols are the same as in Figure 5.

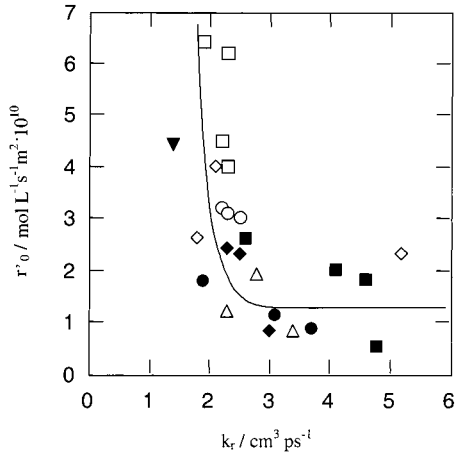

Figure 11. Plot of r'_0 versus k_r values. Symbols are the same as in Figure 5.

values of the initial zero order reaction rates, r_0 and r'_0, of all the samples are reported in Table 1. Here, r'_0 is defined as a zero-order rate constant divided by the BET surface area of the sample.

Figure 10 shows plots of r'_0 as a function of the amount of transition metal loading. Only the samples loaded with tungsten have r'_0 values comparable or higher than that of the pure substrate, TiO_2 HP, with an optimum concentration for TiO_2/W/1. All the other samples show reaction rates rather lower than that of TiO_2 HP, with the exception of TiO_2/Mo/1, the value of which was quite close to that of the support. The powders containing Co, Fe, and V revealed a very scarce photoreactivity and, in particular, the Cr-loaded samples were the least active.

The TOC results after 3 h of irradiation have shown that 4-nitrophenol is completely photodegraded when the bare TiO_2 is used, whereas it is scarcely mineralized in the presence of most of the loaded samples. The extent of mineralization decreases by increasing the content of transition metal.

High mineralization percentages (85−95%) were obtained by employing TiO_2/W/0.3, TiO_2/W/1, and TiO_2/W/2, while a percentage of only ca. 27% was observed for TiO_2/W/5. It is worth noting that 4-nitrophenol was negligibly mineralized in the presence of TiO_2/Mo/2 and TiO_2/Mo/5.

Figure 11 shows the correlation between the initial reaction rates of the various samples and the values of k_r, determined by femtosecond pump−probe diffuse reflection spectroscopy. The k_r values were determined in air, but, as previously reported

for several TiO_2 samples, there is an almost linear relation between values measured in air and in suspension.[41] Although the plot of Figure 11 is fairly scattered, it can be noticed that, by increasing k_r, the rate of 4-nitrophenol disappearance first significantly decreases and then becomes practically constant.

Discussion

The characterization of catalysts prepared by impregnating crystalline TiO_2 powders with various transition metal ions has shown that the photocatalytic behavior of the samples is determined by many physicochemical and intrinsic electronic factors that are difficult to be correlated.

The addition of species of transition metals to polycrystalline TiO_2 is generally detrimental for the photooxidation of organic compounds in solid−liquid reactions.[9] Nevertheless, Hoffmann et al.[43] studied the role of 21 metal ion dopants in quantum-sized TiO_2 and reported that doping with Fe^{3+}, V^{4+}, and Mo^{5+} at 0.1−0.5 atom % significantly enhanced the photoreactivity both for the oxidation of $CHCl_3$ and the reduction of CCl_4, while Co^{3+} decreased the photoreactivity. Likewise, Grätzel and Howe[44] found that doping colloidal TiO_2 particles with Fe, V, and Mo, drastically increased the lifetime of the hole−electron pairs generated by band gap irradiation.

The difference between the photocatalytic behavior of crystalline powders and colloids is not surprising since their surface chemistry is not identical, and furthermore, irradiation of the powders is much less optically efficient because of a more extensive light scattering by the large particles.[44] The photoreactivity of doped quantum-sized TiO_2 appears to be a complex function of the dopant concentration, the energy levels of dopants within the TiO_2 lattice, their d electronic configuration, and the distribution of dopants.[43] The photoactivity of the crystalline powders depends not only on their electronic properties but also on many other factors such as the particle size distribution, the texture, the type of pores present, the different hydroxylation of the surfaces, the acid−base properties, the amount of adsorbed reactant species, etc.

The XRD and SEM results of this work have shown that no significant variations of the structural and morphological habit of the loaded samples compared with the bare TiO_2 can be invoked to explain the observed different photoactivities. The lack of appreciable peaks due to metal oxides in the diffractograms indicates a high degree of dispersion of the loaded metals onto the support, probably because the calcination temperature of the samples is too low to permit the formation of "bulk" oxides.

The presence of small signals attributable to WO_3 in the TiO_2/W/5 sample seems at variance with results reported in previous works claiming that peaks of WO_3 can be observed only for samples containing more than 8 atom % W.[6,45] Regardless, the different amount of metal necessary to detect crystalline WO_3 can be ascribed to the nature of the titania support (TiO_2 HP instead of TiO_2 Degussa P-25)[45] or to the different method used for the preparation of the samples.[6]

The importance of the support is confirmed by the diffractogram of the sample TiO_2/Fe/5, which reveals an anatase/rutile ratio lower than that of bare TiO_2 HP both in its calcined and original forms. This indicates that the starting matrix is modified by the presence of iron as reported also by Navio et al.[46] The incorporation of iron should not catalyze the anatase-to-rutile transformation, at least up to 550 °C[16] but, actually, the ease of phase transformation depends on the nature of the TiO_2 precursor.[47]

The narrow peaks shown by the diffractogram of TiO_2/V/5 suggest an improved crystallization of the powder due probably to an easy diffusion of vanadium ions into the top layers of the support and/or an increase of the particle size. These observations are consistent with the values of surface area of TiO_2/V/2 and TiO_2/V/5, which are low in comparison with most of the other samples.

The specific surface areas of the various samples decrease with increasing the metal loading in the powders, and this effect could be attributed to the obstruction of the pores of the support by metal species. The decrease in area could also originate from a coalescence process since sintering is favored by the presence of dopants.[6, 46] EDX measurements indicate a large scattering of data depending on the location in a single particle, and this insight is in agreement with the above picture. The metal surface composition is generally higher than the nominal one, indicating an enrichment of metallic species on the surface due to an imperfect diffusion of metal ions at the low temperature of preparation, and this is particularly evident for the samples containing molybdenum. On the contrary, the EDX figures are always lower than the nominal ones in the case of the V-loaded samples.

The acidic properties of a metal oxide play an important role in determining its adsorptive and catalytic properties. In dilute binary oxides the major component controls the oxide structure and the dopant surface concentration controls the number of new acid sites.[48] FTIR spectra of ammonia adsorbed on some metal doped titania catalysts have provided evidence of the presence of both Brønsted and Lewis acid sites on the surfaces of the samples.[6,49−53] The Brønsted sites are associated with the presence of the transition metals since they are not detected in pure titania,[54−56] and moreover their concentration generally increases as the metal content increases.

The position of the symmetric deformation bands of coordinately adsorbed ammonia has been related to the strength of the surface Lewis acid sites.[57−59] By comparing the results obtained in previous studies[52−55] the following variation in surface acidity has been proposed:

$$TiO_2/W > TiO_2/Mo > TiO_2/V > TiO_2$$

A similar trend had been previously found for the Brønsted acidity.[60]

The hydrated surface of an oxide exhibits ion exchange properties and there is a correlation between ion exchange capacity and the net surface charge carried by the oxide.[61] An index of the propensity of a surface to become either positively or negatively charged as a function of pH is the point of zero charge which is the value of pH required to give zero net surface charge.

As shown in Figure 4 for the TiO_2/Cr samples, the pzc varies systematically in accordance with the relative content of transition metal. The sequence of the points of zero charge matches rather well with the surface acidity of the samples.

The pzc values of the samples containing Mo, V, and W decrease significantly with increasing the metal content, indicating a surface enrichment of species with an acid behavior as MoO_3, V_2O_5, or WO_3. For the Cr-loaded samples, 0.3 atom % of metal is sufficient to modify strongly the pzc of TiO_2 from 7.1 to 3.6, suggesting the presence of CrO_3 on the surface of the support. As confirmed by XPS studies,[50] the incorporation of appreciable amounts of chromium leads to the formation of surface Brønsted acid sites (Cr^{6+}−OH) whose concentration increases with the chromium content. Probably, the diffractograms of the TiO_2/Cr samples do not reveal any chromium

compound since they are amorphous and/or randomly spread out on the surface of TiO_2 (no evidence of Cr_2O_3 crystallites exists).[15]

The results of 4-nitrophenol photodegradation have shown that loading TiO_2 with Co, Cr, Cu, Fe, Mo, and V causes a decrease of the TiO_2 HP photocatalytic activity, and this effect was more significant as the amount of loaded metal increased. The samples containing tungsten revealed reaction rates higher than that of pure TiO_2, with a maximum between 1 and 2 atom % and a slightly lower photoactivity for TiO_2/W/0.3. These results are in agreement with previous studies performed by using powders prepared by the sol−gel method[6] or by wet impregnation of P-25 Degussa TiO_2.[45] Similarly Wold et al.[5,62] reported a beneficial effect of the presence of tungsten and molybdenum in TiO_2 for the photodegradation of 1,4-dichlorobenzene in aqueous medium.

The photoactivity of the powders roughly decreases according to the following sequence:

$$TiO_2/W > TiO_2/Mo > TiO_2/Cu > TiO_2/Fe \sim TiO_2/Co > TiO_2/V > TiO_2/Cr$$

The acid−base properties of the powders do not strictly correlate with the photoactivity, but they could influence the extent of adsorption of the reacting species on the surface and consequently the photoreactivity. Wold et al.[63] found a relationship between the surface acidity of WO_3/TiO_2 and MO_3/TiO_2 catalysts and their resulting photoefficiency. For these systems, increasing the content of the transition metal increased total acidity. This was attributed to an excess of positive charge caused by the addition of a higher valence cation, such as W^{6+} or Mo^{6+}, on the surface of TiO_2.

For our samples, some general considerations can be done by carefully scrutinizing the pzc values. The surface of the loaded samples with pzc > 4.5, i.e., the pH at which the photoreactivity runs were carried out, acquires an excess of positive charge due to the neutralization of basic sites. On the contrary, when pzc < 4.5, the surface acquires an excess of negative charge due to the neutralization of acidic sites. By the observation of Table 1 it can be noted that the photoactivity of the loaded samples decreases when the pzc is sensibly different from the pH value of 4.5.

The differences in photoactivity between TiO_2 and loaded samples can be also attributed to other characteristics such as the larger particle size or the lower anatase/rutile ratio. Powders with more rutile, such as the TiO_2/Fe samples, could be less active due to the dehydroxylation caused by the anatase-to-rutile phase transformation since dehydroxylation reduces hole trapping by surface hydroxyls, enhancing recombination and oxygen or organic species adsorption. A decrease in the specific surface area can also affect the photoactivity.

The recombination of photogenerated electrons and holes is one of the most significant factors that influence the photoactivity of the samples. The analysis of the decay profiles obtained by femtosecond pump−probe diffuse reflectance spectroscopy indicates that metal loading increases the rate constants of $e^- - h^+$ recombination. The value of k_r markedly increases even at low loading level (0.3%) and furtherly increases along with the amount of transition metal.[14] The sequence of the photoactivities of the various samples is quite in agreement with the values of k_r except for the TiO_2/Cr samples, which have recombination rates intermediate between those of the samples TiO_2/W and TiO_2/Cu.

Figure 11 suggests that the net activity of 4-nitrophenol photodegradation is dominated by the electron−hole recombination rate when the k_r values are relatively low ($k_r < 3$ cm^3 ps^{-1}), whereas the reaction rate becomes independent of k_r when the recombination of the photogenerated pairs is too fast. Obviously the photocatalytic activity of the doped samples is also governed by many other factors, and this justifies also the scattering of the data.

The presence of metal ions does not modify the position of the valence-band edge of anatase which corresponds to the energy of the photogenerated holes and whose value is sufficient to oxidize most organic substrates. This means that bare TiO_2 has the essential conditions for the occurrence of 4-nitrophenol photooxidation because of its suitable oxidation potential and efficient charge separation. Loading influences detrimentally the photoreactivity because it increases the recombination rate of the hole/electron pairs and sometimes modifies unfavorably the diffusion length (l) of the minority carriers. In particular, TiO_2 has $l = 1$ μm, and Cr and V doping lowers respectively the diffusion length to 0.2 and 0.1 μm.[21] Fe and Co give values of 2 μm[21] but, in any case, their presence reduces the photoactivity of TiO_2.

The diffuse reflectance spectra reveal a red shift in the band gap transition, which can be explained by the introduction of energy levels of the transition metal ions into the band gap of TiO_2.[43] Mizushima et al., from optical absorption data and photocurrent measurements, calculated the impurity levels of some iron-group ions in rutile.[64] The presence of such levels was invoked by Grätzel and Howe[44] to explain the role of Fe, V, and Mo on the photoreactivity of TiO_2 colloids.

According to Hoffmann et al.,[43] the presence of energy levels below the conduction band edge and above the valence band edge influences the photoreactivity of TiO_2 since the metal ions can act as electron (or hole) traps altering the electron−hole pair recombination rate. Anyway, these considerations are once more valid for colloid particles where, due to the lack of appreciable band bending, both electrons and holes are readily transferred to the interface to initiate the photoreaction. In large particles the dopants are isolated far from the surface with a low chance of transferring trapped charge carriers to the interface and therefore the metal ions act more likely as recombination centers than as trap sites.[47]

Dopants can affect negatively the photoreactivity of TiO_2, changing the number of active sites, the type or surface groups, and the acid−base properties. The different behavior of the various samples is also related to the solubility of the transition metal in the support, which depends strongly on the radius and the charge of the corresponding ion. Any variation in the electronic structure of the surface is reflected in the adsorption characteristics.

Chromium is the worst dopant among the various metals not only because of its low hole diffusion length[21] but also because the presence of Cr^{3+} ions in lattice positions displacing Ti^{4+} ions introduces electron-acceptor levels positioned about 0.5 eV over the value of the valence band edge.[65] These acceptors are responsible for the decrease in photoconductivity of TiO_2 at every wavelength,[19] since they work as traps for the electrons produced under irradiation.

The Fe−TiO_2 and Co−TiO_2 samples exhibit similar photoactivity, and this seems justifiable since the two metals belong to the same group VIII and have practically the same values of ionic radius ($r_{Fe^{3+}} = 64$ pm, $r_{Co^{3+}} = 63$ pm). On the other hand, the pzc values of the samples containing the same metal loading are very close, and the diffusion length of the holes is the same both for the samples loaded with Fe and for those loaded with Co.[21]

The W-loaded samples are more photoactive than the bare TiO_2 with the exception of TiO_2/W/0.3. These results are in agreement with those obtained previously using impregnated[45] and sol−gel prepared powders.[6] The beneficial effect of W has been explained[5,66] by considering the formation of W(V) species by means of a transfer of photogenerated electrons from TiO_2 to W(VI). Subsequently W(V) could be oxidized to W(VI) by transferring electrons to adsorbed O_2.[6]

The X-ray results have indicated the presence of small amounts of WO_3 on the surface of the catalysts. The localized heterojunctions formed by the contact between two chemically distinct phases and/or the interface acceptor states can improve the separation of the photogenerated pairs and, consequently, could be responsible for the observed higher photoactivity.[6]

It cannot be excluded that tungsten species in the TiO_2 lattice could act as recombination centers for the electron−hole pair recombination according to the following reactions:

$$W^{6+} + e^- \rightarrow W^{5+}$$

$$W^{5+} + h^+ \rightarrow W^{6+}$$

These reactions are in competition with the redox processes that can occur at the solid/liquid interface and could play a significant role for the lightest loaded sample, TiO_2/W/0.3, negatively influencing its photoactivity.[6]

Although the k_r or pzc values (see Table 1) cannot justify the enhanced observed photoactivity since all the properties contribute on various extent to it, it is worth noting that the k_r values of the TiO_2/W powders are not too high compared with that of the support. Moreover, TiO_2/W/1, which exhibits the highest photoreactivity, presents one of the lowest k_r values among all the loaded samples. As far as the pzc values are concerned, TiO_2/W/0.3 and TiO_2/W/5 have k_r values comparable with those of the other W-loaded samples, but their point of zero charge is somewhat different from 4.5 and this could justify their lower photoactivity.

As regards the mineralization of 4-nitrophenol, the TOC determinations have revealed that the bare TiO_2 is more efficient than each of the loaded samples. The explanation could be found in a less significant interaction between the surface of the loaded catalysts and the intermediate species produced during the reaction of photodegradation.

The negligible extent of mineralization observed in the presence of TiO_2/Mo/2 and TiO_2/Mo/5 could be ascribed to the relatively slight tendency of molybdenum to diffuse into the TiO_2 lattice, as suggested by the EDX measurements, which have revealed amounts of metal higher than the nominal values. The presence of molybdenum surface species could not favor the photoabsorption of the reacting species and a similar interpretation can be valid also for TiO_2/W/5. The low mineralization percentage obtained with this last W-loaded sample can be attributed to a high coverage of the surface of TiO_2 particles with "bulk" WO_3.

It is worth noting that doped TiO_2 samples can show different efficiency with respect to the photodegradation of different substrates. For example, the presence of molybdenum species has been found beneficial for the photocatalytic activity of TiO_2 in the oxidation of 1,4-dichlorobenzene,[62,63] different from what was observed in the case of 4-nitrophenol.

The apparent contrasting results obtained with the samples containing vanadium, i.e., slight photoactivity and relatively low amounts of metal species present on the surfaces, suggest that the physicochemical surface characteristics play a role that is less important than the other physical and intrinsic electronic factors.

Acknowledgment. The authors thank the Ministero dell'Università e della Ricerca Scientifica e Tecnologica (Italy) and the Ministry of Education, Science, Sports and Culture (Japan) for financial support. Dr. Hidenori Noguchi (Hokkaido University, presently Tokyo Institute of Technology) is gratefully acknowledged for his help in PP-DRS measurements.

References and Notes

(1) *Homogeneous and Heterogeneous Photocatalysis*; Pelizzetti E., Serpone N., Eds.; Reidel: Dordrecht, The Netherlands, 1986.

(2) *Photocatalysis and Environment: Trends and Applications*; Schiavello, M., Ed.; Kluwer Academic Publishers: Dordrecht, The Netherlands, 1988.

(3) *Photocatalysis: Fundamentals and Applications*; Pelizzetti E., Serpone N., Eds.; Wiley: New York, 1989.

(4) Soria, J.; Conesa, J. C.; Augugliaro, V.; Palmisano, L.; Schiavello, M.; Sclafani, A. *J. Phys. Chem.* **1991**, *95*, 275 and references therein.

(5) Do, Y. R.; Lee, W.; Dwight, K.; Wold, A. *J. Solid State Chem.* **1994**, *108*, 198.

(6) Marcì, G.; Palmisano, L.; Sclafani, A.; Venezia, A. M.; Campostrini, R.; Carturan, G.; Martin, C.; Rives, V.; Solana, G. *J. Chem. Soc., Faraday Trans.* **1996**, *92*, 819.

(7) Yamashita, H.; Nishiguchi, H.; Kamada, N.; Anpo, M.; Teraoka, Y.; Hatano, H.; Ehara, S.; Kikui, K.; Palmisano, L.; Sclafani, A.; Schiavello, M.; Fox, M. A. *Res. Chem. Intermed.* **1994**, *20*, 815.

(8) Anpo, M. *Catal. Surv. Jpn.* **1997**, *1*, 169.

(9) Palmisano L.; Sclafani A. In *Heterogeneous Photocatalysis, Wiley Series*: *Photoscience and Photoengineering*; Schiavello, M., Ed.; John Wiley & Sons: Chichester, 1997; Vol. 3, Chapter 4, p 109 and references therein.

(10) Memming, R. In *Photoelectrochemistry, Photocatalysis and Photoreactors*; Schiavello, M., Ed.; Reidel: Dordrecht, 1985; p 107.

(11) Lee, P. C.; Meisel, D. *J. Catal.* **1981**, *70*, 160.

(12) Wang, C. M.; Heller, A.; Gerischer, H. *J. Am. Chem. Soc.* **1992**, *114*, 5230.

(13) Sclafani, A.; Palmisano, L.; Marcì G.; Venezia, A. M. *Sol. Energy Sol. Cells* **1998**, *51*, 203.

(14) Ikeda, S.; Sugiyama, N.; Pal, B.; Marcì, G.; Palmisano, L.; Noguchi, H.; Uosaki, K.; Ohtani, B. *Phys. Chem. Chem. Phys.* **2001**, *3*, 267.

(15) Palmisano, L.; Augugliaro, V.; Sclafani A.; Schiavello, M. *J. Phys. Chem.* **1988**, *92*, 6710.

(16) Palmisano, L.; Schiavello, M.; Sclafani, A.; Martin, C.; Martin I.; Rives, V. *Catal. Lett.* **1994**, *24*, 303.

(17) Martin, C.; Martin, I.; Rives, V.; Palmisano, L.; Schiavello, M. *J. Catal.* **1992**, *134*, 434.

(18) Litter I.; Navio, J. A. *J. Photochem. Photobiol. A: Chem.* **1996**, *98*, 171.

(19) Herrmann, J. M.; Disdier, J.; Pichat, P. *Chem. Phys. Lett.* **1984**, *108*, 618.

(20) Wilke K.; Breuer, H. D. *J. Photochem. Photobiol. A: Chem.* **1999**, *121*, 49.

(21) Maruska, H. P.; Ghosh, A. K. *Sol. Energy Mater.* **1979**, *1*, 237.

(22) Anpo, M.; Ichihashi, Y.; Takeuchi M.; Yamashita, H. *Res. Chem. Intermed.* **1998**, *24*, 143.

(23) Anpo, M.; Ichihashi, Y.; Takeuchi M.; Yamashita H. In *Science and Technology Catalysis 1998*; Delmon, B., Yates, J. T., Eds.; Kodansha: Tokyo, 1999; p 305.

(24) Sakata, T.; Kawai T.; Hashimoto, K. *Chem. Phys. Lett.* **1982**, *88*, 131.

(25) Harada H.; Veda, T. *Chem. Phys. Lett.* **1984**, *106*, 229.

(26) Ohtani, B.; Handa, J.; Nishimoto, S.; Kagiya, T. *Chem. Phys. Lett.* **1985**, 120, 292.

(27) Sclafani, A.; Palmisano L.; Schiavello, M. *J. Phys. Chem.* **1990**, *94*, 829.

(28) Augugliaro, V.; Palmisano, L.; Schiavello, M.; Sclafani, A.; Marchese, L.; Martra G.; Miano, F. *Appl. Catal.* **1991**, *69*, 323.

(29) Bosch, H.; Peppelenbos, E. *J. Phys. E* **1977**, *10*, 605.

(30) Subramanian, S.; Noh, J. S.; Schwarz, J. A. *J. Catal.* **1988**, *114*, 433.

(31) Noh, J. S.; Schwarz, J. A. *J. Colloid Interface Sci.* **1989**, *130*, 157.

(32) Brady, R. L.; Southmayd, D.; Contescu, C.; Zhang R.; Schwarz, J. A. *J. Catal.* **1991**, *129*, 195.

(33) JCPDS files Nos. 21−1275 and 21−1276.

(34) Spurr, R. A.; Mayers, H. *Anal. Chem.* **1957**, *29*, 760.

(35) JCPDS file No. 5-0363.

(36) Stumm, W.; Morgan, J. J. *Aquatic Chemistry*, 2nd ed.; Wiley: New York, 1981; p 632.

(37) Takahashi, K.; Tagaya, H. T.; Higashitsuji, K.; Kittaka, S. In *Electrical Phenomena at Interfaces*; Kitahara A., Watanabe A., Eds.; Marcel Dekker: New York, 1984; Chapter 6.

(38) Lyklema, J. *J. Colloid Interface Sci.* **1984**, *99*, 109.

(39) Colombo, D. P., Jr.; Bowman, R. M. *J. Phys. Chem*. **1995**, *99*, 11752.
(40) Colombo, D. P., Jr.; Bowman, R. M. *J. Phys. Chem*. **1996**, *100*, 18445.
(41) Ohtani, B.; Kominami, H.; Bowman, R. M.; Colombo, D. P., Jr.; Noguchi H.; Uosaki, K. *Chem. Lett.* **1998**, 579.
(42) Colombo, D. P., Jr.; Roussel, K. A.; Saeh, J.; Skinner, D. E.; Cavaleri, J. J.; Bowman, R. M. *Chem. Phys. Lett.* **1995**, *232*, 207.
(43) Choi, W.; Termin, A.; Hoffmann, M. R. *J. Phys. Chem*. **1994**, *98*, 13669.
(44) Graetzel, M.; Howe, R. F. *J. Phys. Chem*. **1990**, *94*, 2566.
(45) Martin, C.; Solana, G.; Rives, V.; Marcì, G.; Palmisano, L.; Sclafani, A. *Catal. Lett.* **1997**, *49*, 235.
(46) Navio, J. A.; Colón, G.; Bitter, M. I.; Bianco, G. N. *J. Mol. Catal. A: Chemistry* **1996**, *106*, 267.
(47) Litter, M. I.; Navio, J. A. *J. Photochem. Photobiol. A: Chem*. **1996**, *99*, 1.
(48) Connell, G.; Dumesic, J. A. *J. Catal*. **1987**, *105*, 285.
(49) del Arco, M.; Martín, C.; Rives, V.; Sánchez-Escribano, V.; Ramis, G.; Busca, G.; Lorenzelli, V.; Malet, P. *J. Chem. Soc., Faraday Trans*. **1993**, *89*, 1071.
(50) Venezia, A. M.; Palmisano, L.; Schiavello, M.; Martin, C.; Martin, I.; Rives, V. *J. Catal*. **1994**, *147*, 115.
(51) Palmisano, L.; Schiavello, M.; Sclafani, A.; Martin, C.; Martin, I.; Rives, V. *Catal. Lett.* **1994**, *24*, 303.
(52) Ramis, G.; Busca, G.; Bregani, F.; Forzatti, P. *Appl. Catal*. **1990**, *64*, 259.
(53) Ramis, G.; Busca, G.; Cristiani, C.; Lietti, L.; Forzatti, P.; Bregani, F. *Langmuir* **1992**, *8*, 1744.
(54) Busca, G.; Saussey, H.; Saur, O.; Lavalley, J. C.; Lorenzelli, V. *Appl. Catal*. **1985**, *14*, 245.
(55) Ramis, G.; Busca, G.; Lorenzelli, V.; Forzatti, P. *Appl. Catal*. **1990**, *64*, 243.
(56) Miyata, H.; Nakagawa, Y.; Ono, T.; Kubokawa, Y. *J. Chem. Soc., Faraday Trans. 1* **1983**, *79*, 2343.
(57) Tsyganenko, A. A.; Pozdnyakov, D. V.; Filiminov, V. N. *J. Mol. Struct*. **1975**, *29*, 299.
(58) Nakamoto, K. *Infrared and Raman Spectra of Inorganic and Coordination Compounds*, 4th ed.; Wiley: New York, 1986.
(59) Davydov, A. A. *Infrared Spectroscopy of Adsorbed Species on the Surface of Transition Metal Oxides*; Wiley: New York, 1990.
(60) Ramis, G.; Busca, G.; Lorenzelli, V. In *Structure and Reactivity of Surfaces*; Zecchina, A., Costa, V., Morterra, C., Eds.; Elsevier: Amsterdam, 1989; p 77.
(61) James, R. O. *Adsorption of Inorganics at Solid Interfaces*; Anderson M. A., Rubin, A. J., Eds.; Ann Arbor Science: Ann Arbor, 1981; Chapter 6.
(62) Lee, W.; Do, Y. R.; Dwight, K.; Wold, A. *Mater. Res. Bull*. **1993**, *28*, 1127.
(63) Papp, J.; Soled, S.; Dwight, K.; Wold, A. *Chem. Mater*. **1994**, *6*, 496.
(64) Mizushima, K.; Tanaka, M.; Asai, A.; Iida, S.; Goodenough, J. B. *J. Phys. Chem. Solids* **1979**, *40*, 1129.
(65) Ghosh, A. K.; Maruska, H. P. *J. Electrochem. Soc.* **1977**, *124*, 1516.
(66) Tennakone, K.; Heperuma, O. A.; Bandara, J. M. S.; Kiridena, W. C. B. *Semicond. Sci. Technol*. **1992**, *7*, 423.